
Adaptive Braking for Mitigating Gradient Delay

Abhinav Venigalla^{*1} Atli Kosson^{*1} Vitaliy Chiley¹ Urs Köster²

Abstract

Neural network training is commonly accelerated by using multiple synchronized workers to compute gradient updates in parallel. Asynchronous methods remove synchronization overheads and improve hardware utilization at the cost of introducing gradient delay, which impedes optimization and can lead to lower final model performance. We introduce Adaptive Braking (AB), a modification for momentum-based optimizers that mitigates the effects of gradient delay. AB dynamically scales the gradient based on the alignment of the gradient and the velocity. This can dampen oscillations along high curvature directions of the loss surface, stabilizing and accelerating asynchronous training. We show that applying AB on top of SGD with momentum enables training ResNets on CIFAR-10 and ImageNet-1k with delays exceeding 32 update steps with minimal drop in final test accuracy.

1. Introduction

Computational workloads for training state-of-the-art deep learning models have grown rapidly in recent years (Amodei & Hernandez, 2018). This growth has outpaced the growth in compute power available on individual accelerators. To keep training times manageable, these workloads are often distributed over a cluster of devices working in parallel. The most common form of distributed training is Distributed Synchronized SGD (Chen et al., 2016) which divides a mini-batch of samples between workers and accumulates the gradients from all workers before updating the model parameters. The workers are synchronized and can not start processing the next mini-batch until the weights have been updated which lowers hardware utilization.

^{*}Equal contribution ¹Cerebras Systems, Los Altos, CA ²Google, San Diego, CA, work done while at Cerebras Systems. Correspondence to: Abhinav Venigalla <abhi@cerebras.net>, Atli Kosson <atli@cerebras.net>.

Lian et al. (2015) propose performing asynchronous weight updates to avoid the synchronization overhead. Asynchronous weight updates can improve hardware utilization at the cost of introducing gradient delay (Lian et al., 2015). The effects of gradient delay have been studied in several works. Yang et al. (2019) show that delays cause unstable oscillations in the optimization trajectory lowering the maximum stable learning rate. Mitliagkas et al. (2016) show that delays with a particular distribution can increase the effective momentum in the underlying optimization process. Giladi et al. (2020) and Kosson et al. (2020) suggest that gradient delay removes the benefits of momentum and that with delays momentum should only be used if modified. Without mitigation, gradient delay commonly results in slower optimization and worse final model performance (Chen et al., 2016). Many methods have been proposed to improve convergence with gradient delay (Hakimi et al., 2019; Zhang et al., 2016; Zheng et al., 2017; Guan et al., 2017; Rigazzi, 2019; Giladi et al., 2020).

Adaptive Braking (AB) is a modification to the momentum update process that can greatly increase tolerance to delayed gradients with minimal compute overhead and no memory overhead. AB dynamically scales the gradient magnitude based on the angle between the gradient and velocity vectors, decreasing it for positive alignment (acute angle) and increasing it for negative alignment (obtuse angle). Intuitively AB can dampen oscillations along a single gradient component by reducing the velocity magnitude at every step. In the case of multiple components with different, constant, curvatures, the alignment of the gradient and velocity will be more strongly correlated with the high curvature components. This means that AB primarily dampens oscillations for the components with high curvature, stabilizing them without affecting the other components as much on average. This resembles the effect of higher order optimization methods which account for the loss landscape curvature.

In this work we focus on applying AB to Stochastic Gradient Descent with Momentum (SGDM). We show that training with SGDM+AB can improve asynchronous multi-worker training in multiple settings with no tuning of the single-worker hyperparameters. In particular, SGDM+AB enables training ResNet-20 on CIFAR-10 and ResNet-50 on ImageNet-1k with large delays $D \geq 32$ with minimal accuracy degradation. In our experiments we compare AB with

several other mitigation methods showing that AB enables greater delay tolerance than other methods.

2. Algorithm

Adaptive Braking (AB) is a general technique for momentum-based optimizers. It computes a gradient-velocity alignment score and uses it to scale the gradient. In this section we describe how AB is applied to SGDM.

The original SGDM update is:

$$\mathbf{v}_{t+1} = m\mathbf{v}_t + \mathbf{g}_t \quad (1)$$

$$\mathbf{w}_{t+1} = \mathbf{w}_t - \eta\mathbf{v}_{t+1} \quad (2)$$

where \mathbf{w}_t and \mathbf{v}_t are the model weights and velocity at time t , η is the learning rate, and m is the momentum coefficient. The weight gradient applied at time t is \mathbf{g}_t which may have been computed with a delay, $\mathbf{g}_t = G(\mathbf{w}_{t-D})$, where $G(\cdot)$ is the gradient function and D is a random variable representing the system delay.

In (1) and (2), each weight parameter is independent and can be processed separately. Adaptive Braking groups parameters so that it can compute a gradient-velocity alignment per group. By default we use a filter-wise grouping of parameters as described in Appendix D.

To apply Adaptive Braking, we compute the gradient scaling factor α_t^i based on the cosine similarity of the velocity and gradient vectors for parameter group i . The SGDM+AB update is:

$$\alpha_t^i = 1 - \rho \frac{\langle \mathbf{g}_t^i, \mathbf{v}_t^i \rangle}{\max(\|\mathbf{g}_t^i\| \|\mathbf{v}_t^i\|, \epsilon)} \quad (3)$$

$$\approx 1 - \rho \cos \angle(\mathbf{g}_t^i, \mathbf{v}_t^i) \quad (4)$$

$$\mathbf{v}_{t+1}^i = m\mathbf{v}_t^i + \alpha_t^i \mathbf{g}_t^i \quad (4)$$

$$\mathbf{w}_{t+1}^i = \mathbf{w}_t^i - \eta\mathbf{v}_{t+1}^i \quad (5)$$

where ρ is a scalar hyperparameter we call the *braking coefficient* (Appendix G), and ϵ is used for numerical stability. Different formulations of Adaptive Braking could substitute the cosine similarity with other distance functions.

3. Optimizing a Noisy Quadratic Model

To gain insights into how AB can help optimization, we analyze its effect on convergence for a Noisy Quadratic Model (NQM). We adopt the setup that Zhang et al. (2019) used to model the effects of batch size in neural networks. The NQM allows us to explicitly control various aspects of the optimization such as the dimensionality, the amount of noise, the condition number, and the delay. We measure

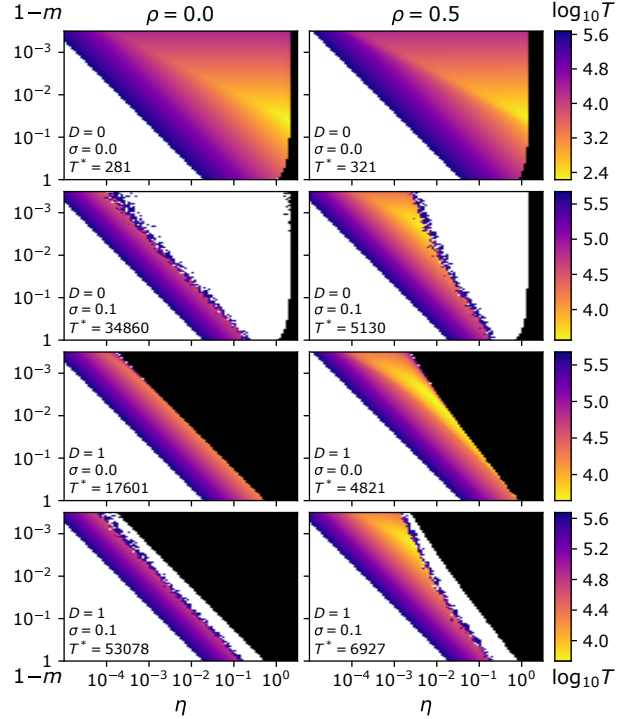


Figure 1. This figure shows the number of optimization steps, T , required to reach the target loss on the NQM from Section 3 for different hyperparameters. Each heatmap plots T over different learning rates η and momentum m . Black regions are unstable and white regions to not reach the target loss within the 500000 steps performed. The left column shows SGDM and the right column shows Adaptive Braking with $\rho = 0.5$. The rows show different amounts of delay D and noise σ . T^* estimates the fastest trajectory based on the 1st percentile of T over the colored region (to reduce the effects of noise and the choice of sampling grid).

the quality of optimization trajectories by the number of optimization steps, T , required to reach a target loss. See Appendix K.1 for details about our setup.

Figure 1 compares T for SGDM with and without AB for different learning rates, momentum values, delay and noise. The first row shows the no-delay and no-noise case. In this case AB does not improve the speed and slightly decreases the highest stable learning rate. This happens because AB can magnify certain high-frequency oscillations, where g and v are almost always oppositely aligned, causing AB to effectively scale the learning rate by up to $1 + \rho$. Appendix K.3 explores this effect further and shows how AB can be modified to avoid this.

The results of adding noise in the no-delay case are shown in the second row of Figure 1. In this case AB significantly speeds up the fastest trajectory and expands the region that reaches the target loss within the step budget. In the presence of noise, a constant learning rate trajectory will converge to an expected steady-state loss that depends on the hyperparameters and level of noise. Zhang et al. (2019)

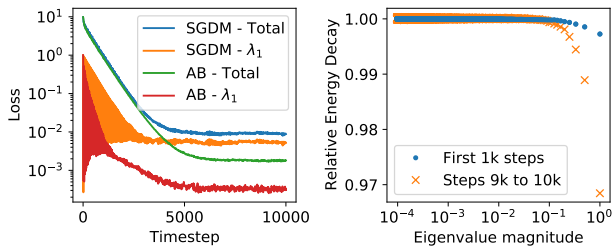


Figure 2. AB can lower the steady state loss when optimizing a noisy quadratic model. The learning rate and momentum correspond to values that reach the target loss (10^{-2}) with AB but not SGDM in the second row of Figure 1. **Left:** The total loss in each case and the contribution to the loss from the largest eigenvalue. The steady-state loss for the largest eigenvalues is lower with AB. **Right:** The relative energy decay ratio for each eigenvalue showing a greater dampening of high curvature components.

show that there is a trade-off with increasing the momentum and/or learning rate: it can improve the convergence rate (of the expectation) but magnifies the steady-state loss. The dampening effect of AB can reduce the steady-state loss, expanding the region that will converge within the time limit and unlocking the faster trajectories with larger step sizes. To measure the dampening effect of AB we can compare the energy after making an AB update (E_{t+1}) to what the energy would have been after making a SGDM update (\hat{E}_{t+1}) from each state $(\mathbf{w}_t, \mathbf{v}_t)$ along the AB optimization trajectory. The energy $E_t = \mathcal{L}(\mathbf{w}_t) + \frac{1}{2}\eta\|\mathbf{v}_t\|^2$ accounts for both potential energy (the loss $\mathcal{L}(\mathbf{w}_t)$) and kinetic energy $\frac{1}{2}\eta\|\mathbf{v}_t\|^2$ of an optimization state (see Appendix K.2). The geometric mean of E_{t+1}/\hat{E}_{t+1} , which we call the *relative energy decay*, indicates how much faster AB dissipates energy compared to SGDM on average. The relative energy decay can be computed for each eigenvector to measure the dampening for different components. Figure 2 shows that AB can lower the steady state-loss by dampening the large eigenvalue components.

The third and fourth rows of Figure 1 show that AB can help with gradient delay. AB can expand the region of convergence and significantly reduce the time required to reach the target loss. Similar to Kosson et al. (2020), we note that standard momentum does not seem to help in the delay case but with AB there can be a significant benefit. Delays intuitively cause optimization to overshoot, introducing and amplifying oscillations. AB seems to help stabilize these oscillations improving convergence in the presence of gradient delay. Figure 3 explores this effect. It shows that AB can dampen high curvature components stabilizing training with gradient delay.

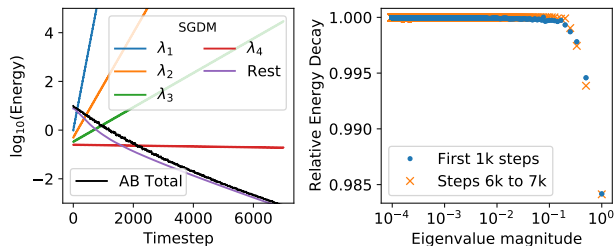


Figure 3. AB can stabilize training with gradient delay. The learning rate and momentum correspond to values that reach the target loss with AB but are unstable for SGDM in the third row of Figure 1. **Left:** The components corresponding to the three largest eigenvalues are unstable without AB. **Right:** AB dissipates energy in these components on average which stabilizes training.

4. Training Neural Networks

To measure the effectiveness of AB for training neural networks with gradient delay, we simulate multi-worker ASGD. We do this on a single machine by storing a history of the master weights $[\mathbf{w}_t, \mathbf{w}_{t-1}, \mathbf{w}_{t-2} \dots \mathbf{w}_{t-D}]$. We then use a chosen algorithm to compute the updated master weights \mathbf{w}_{t+1} using the delayed gradient $\mathbf{g}_t = G(\mathbf{w}_{t-D})$. In all experiments we use a constant delay D , which is representative of an ideal ASGD setting with $D+1$ workers and round robin scheduling. All experiments were implemented using the PyTorch framework (Paszke et al., 2019), and executed on NVIDIA T4 or V100 GPUs.

The main metric we are interested in is the final test accuracy of our trained model compared to a zero-delay, single-worker SGDM baseline. This baseline represents the best possible convergence scenario albeit with no parallelism and no speedup. We evaluate the delay tolerance of algorithms by comparing how much the final test accuracy degrades when training with ASGD and different delays D . For consistency, we do not change the per-worker hyperparameters from the original SGDM baseline. We report experiments on two common image classification tasks: ResNet-20 trained on CIFAR-10 (Krizhevsky, 2009) and ResNet-50 trained on ImageNet-1k (Krizhevsky et al., 2012). Hyperparameter settings can be found in Appendix B.

In addition to Adaptive Braking, we also evaluate and compare against a variety of gradient delay mitigation strategies¹: Shifted Momentum (SM) (Giladi et al., 2020), DANA (Hakimi et al., 2019), Delay-Compensation (DC) (Zheng et al., 2017), and Staleness-Aware (SA) (Zhang et al., 2016).

¹Algorithmic details can be found in Appendix A.

4.1. CIFAR-10

In Figure 4, we simulate asynchronous training of ResNet-20 on CIFAR-10. We evaluate SGDM combined with other delay mitigation strategies and compare them against SGDM+AB with $\rho = 2$ (hyperparameter search shown in Appendix C). We find that training with SGDM+AB leads to equivalent accuracy at small-to-moderate delays, and significantly outperforms the other mitigation strategies at large delays ($D = 128$). We also see more stability from run-to-run when compared to the other strategies.

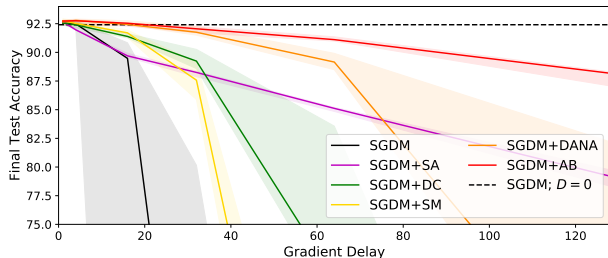


Figure 4. ResNet-20 + CIFAR-10 final test accuracy vs delay. AB provides greater delay tolerance than other mitigation strategies. Each line shows the median over five trials.

To gain further insight into AB’s effects, we measure key metrics α_t^i and $\|\mathbf{v}_t^i\|$ during CIFAR-10 training and discuss their implications in Appendices G and H, respectively.

4.2. ImageNet-1k

In Figure 5, we simulate asynchronous training of ResNet-50 on ImageNet-1k with a delay of $D = 32$. We compare the vanilla SGDM optimizer to SGDM+AB with $\rho = 2$. For our zero-delay baseline, in addition to using a single worker as in the CIFAR-10 experiments, we also include a more realistic Synchronous SGD (SSGD) setup with $D + 1 = 33$ workers. For the SSGD run we use a large batch size of $BS' = 32 * 33 = 1056$ and linearly-scaled learning rate $LR' = 0.00125 * 33 = 0.04125$.

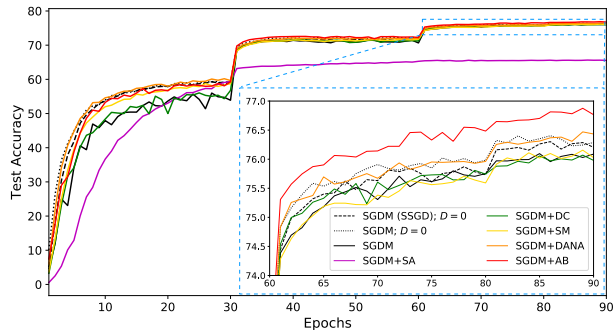


Figure 5. AB outperforms other delay mitigation strategies when training ResNet-50 on ImageNet with a delay of $D = 32$.

We confirm that training with vanilla SGDM and gradient

Table 1. ResNet-50 + ImageNet-1k final test accuracy. The median value over the last 5 epochs is reported.

ALGORITHM	BS	D	ACCURACY	DEGRADATION
SGDM	32	0	76.29%	—
SGDM (SSGD)	1056	0	76.27%	-0.02%
SGDM	32	32	76.05%	-0.24%
SGDM+SA	"	"	65.59%	-10.70%
SGDM+DC	"	"	75.99%	-0.30%
SGDM+SM	"	"	76.05%	-0.24%
SGDM+DANA	"	"	76.38%	+0.09%
SGDM+AB	"	"	76.81%	+0.52%

delay leads to poor convergence at the start of training, and a final test accuracy degradation of -0.24% compared to the single-worker baseline. Using SGDM+AB leads to more stable convergence during early training; the test accuracy curve is closer to synchronous training. Overall, AB prevents final accuracy degradation for asynchronous training and even outperforms the single-worker baseline by +0.52%.

We also compare AB with other delay mitigation strategies in the same ASGD setting. We find that SGDM+AB outperforms the other algorithms in terms of final test accuracy. Among the other algorithms, SGDM+DANA performs the best, and following a similar trajectory to AB in the early stages of training. Final test accuracies for all methods are reported in Table 1.

5. Conclusion

Adaptive Braking scales the gradient based on the alignment of the gradient and velocity. This is a non-linear operation that dampens oscillations along the high-curvature components of the loss surface without affecting the other components much on average. It is especially effective in the presence of gradient delay where it can stabilize components that would otherwise be unstable. We show that AB is competitive with state of the art methods for ASGD training.

The increased delay tolerance that AB provides could enable hardware speedups for both data-parallel distributed training as well as pipeline-parallel training with pipelined backpropagation (Pérowski et al., 1993; Chen et al., 2012; Harlap et al., 2018).

In this work we have focused on the SGDM optimizer, but future work could propose similar modifications to other optimizers such as Adam (Kingma & Ba, 2014).

Acknowledgements

We thank Joel Hestness, Vithursan Thangarasa, and Xin Wang for their help and feedback that improved the manuscript.

References

- Amodei, D. and Hernandez, D. AI and compute. *Heruntergeladen von <https://blog.openai.com/aiand-compute>*, 2018.
- Chen, C.-C., Yang, C.-L., and Cheng, H.-Y. Efficient and robust parallel dnn training through model parallelism on multi-gpu platform. *arXiv preprint arXiv:1809.02839*, 2018.
- Chen, J., Pan, X., Monga, R., Bengio, S., and Jozefowicz, R. Revisiting distributed synchronous sgd. *arXiv preprint arXiv:1604.00981*, 2016.
- Chen, X., Eversole, A., Li, G., Yu, D., and Seide, F. Pipelined back-propagation for context-dependent deep neural networks. In *Interspeech*. ISCA, September 2012.
- Giladi, N., Nacson, M. S., Hoffer, E., and Soudry, D. At stability’s edge: How to adjust hyperparameters to preserve minima selection in asynchronous training of neural networks? In *International Conference on Learning Representations*, 2020.
- Guan, N., Shan, L., Yang, C., Xu, W., and Zhang, M. Delay compensated asynchronous adam algorithm for deep neural networks. In *2017 IEEE International Symposium on Parallel and Distributed Processing with Applications and 2017 IEEE International Conference on Ubiquitous Computing and Communications (ISPA/IUCC)*, pp. 852–859, Dec 2017. doi: 10.1109/ISPA/IUCC.2017.00130.
- Hakimi, I., Barkai, S., Gabel, M., and Schuster, A. DANA: Scalable out-of-the-box distributed ASGD without retuning, 2019.
- Harlap, A., Narayanan, D., Phanishayee, A., Seshadri, V., Devanur, N. R., Ganger, G. R., and Gibbons, P. B. PipeDream: Fast and efficient pipeline parallel dnn training. *ArXiv*, abs/1806.03377, 2018.
- Hermans, J. and Louppe, G. Gradient energy matching for distributed asynchronous gradient descent. *arXiv preprint arXiv:1805.08469*, 2018.
- Kingma, D. P. and Ba, J. Adam: A method for stochastic optimization. *arXiv preprint arXiv:1412.6980*, 2014.
- Kosson, A., Chiley, V., Venigalla, A., Hestness, J., and Köster, U. Pipelined backpropagation at scale: Training large models without batches. *arXiv preprint arXiv:2003.11666*, 2020.
- Krizhevsky, A. Learning multiple layers of features from tiny images. Technical report, 2009.
- Krizhevsky, A., Sutskever, I., and Hinton, G. E. Imagenet classification with deep convolutional neural networks. In Pereira, F., Burges, C. J. C., Bottou, L., and Weinberger, K. Q. (eds.), *Advances in Neural Information Processing Systems 25*, pp. 1097–1105. Curran Associates, Inc., 2012.
- Lian, X., Huang, Y., Li, Y., and Liu, J. Asynchronous parallel stochastic gradient for nonconvex optimization. In Cortes, C., Lawrence, N. D., Lee, D. D., Sugiyama, M., and Garnett, R. (eds.), *Advances in Neural Information Processing Systems 28*, pp. 2737–2745. Curran Associates, Inc., 2015.
- Mitliagkas, I., Zhang, C., Hadjis, S., and Ré, C. Asynchrony begets momentum, with an application to deep learning. In *2016 54th Annual Allerton Conference on Communication, Control, and Computing (Allerton)*, pp. 997–1004. IEEE, 2016.
- ODonoghue, B. and Candes, E. Adaptive restart for accelerated gradient schemes. *arXiv preprint arXiv:1204.3982*, 2012.
- Paszke, A., Gross, S., Massa, F., Lerer, A., Bradbury, J., Chanan, G., Killeen, T., Lin, Z., Gimelshein, N., Antiga, L., Desmaison, A., Kopf, A., Yang, E., DeVito, Z., Raison, M., Tejani, A., Chilamkurthy, S., Steiner, B., Fang, L., Bai, J., and Chintala, S. Pytorch: An imperative style, high-performance deep learning library. In *Advances in Neural Information Processing Systems 32*, pp. 8024–8035. Curran Associates, Inc., 2019.
- Pétrowski, A., Dreyfus, G., and Girault, C. Performance analysis of a pipelined backpropagation parallel algorithm. *IEEE transactions on neural networks*, 4 6:970–81, 1993.
- Rigazzi, A. Dc-s3gd: Delay-compensated stale-synchronous sgd for large-scale decentralized neural network training. In *2019 IEEE/ACM Third Workshop on Deep Learning on Supercomputers (DLS)*, pp. 62–68, 2019.
- Shallue, C. J., Lee, J., Antognini, J., Sohl-Dickstein, J., Frostig, R., and Dahl, G. E. Measuring the effects of data parallelism on neural network training. *Journal of Machine Learning Research*, 20(112):1–49, 2019.
- Yang, B., Zhang, J., Li, J., Ré, C., Aberger, C. R., and De Sa, C. Pipemare: Asynchronous pipeline parallel dnn training. *arXiv preprint arXiv:1910.05124*, 2019.

Zhang, G., Li, L., Nado, Z., Martens, J., Sachdeva, S., Dahl, G., Shallue, C., and Grosse, R. B. Which algorithmic choices matter at which batch sizes? insights from a noisy quadratic model. In *Advances in Neural Information Processing Systems*, pp. 8194–8205, 2019.

Zhang, W., Gupta, S., Lian, X., and Liu, J. Staleness-aware async-sgd for distributed deep learning. In *Proceedings of the Twenty-Fifth International Joint Conference on Artificial Intelligence, IJCAI16*, pp. 2350–2356. AAAI Press, 2016. ISBN 9781577357704.

Zheng, S., Meng, Q., Wang, T., Chen, W., Yu, N., Ma, Z.-M., and Liu, T.-Y. Asynchronous stochastic gradient descent with delay compensation. In *Proceedings of the 34th International Conference on Machine Learning - Volume 70, ICML'17*, pp. 4120–4129. JMLR.org, 2017.

A. Related Work

Asynchronous methods are used to improve compute utilization for neural network training but introduce gradient staleness. Gradients are stale because the gradient is computed using weight from D time steps ago, $\mathbf{g}_t = G(\mathbf{w}_{t-D})$. To mitigate this Giladi et al. (2020) propose adding delay to the velocity as well, \mathbf{v}_{t-D} . They do this by tracking an independent velocity for each worker and updating the master weights using the current worker’s velocity. Another class of mitigation strategies attempts to predict future weights $\hat{\mathbf{w}}_{t-D} \approx \mathbf{w}_t$ for use in the gradient computation, $\mathbf{g}_t = G(\hat{\mathbf{w}}_{t-D})$. Most methods (Chen et al., 2018; Hakimi et al., 2019; Kosson et al., 2020) use the velocity vector to estimate the future weights.

Zhang et al. (2016) propose Staleness-Aware (SA) and show that down-weighting the gradients based on the delay D (gradient penalization) can improve asynchronous training. Kosson et al. (2020) characterize the impulse response of gradients in the optimization process and modify the delayed impulse response to match the non-delayed setting in a technique called Spike Compensation.

Delay Compensated ASGD (Zheng et al., 2017) and its variants (Guan et al., 2017; Rigazzi, 2019) estimate the gradient using the first two terms of the Taylor expansion of the delayed gradient function. Using the Taylor expansion of the delayed gradient function requires estimating the Hessian and storing the old weights. Applying DC-ASGD with a velocity approximation for the weight change is closely related to element-wise Adaptive Braking (See Appendix F).

ODonoghue & Candes (2012) use a method called Adaptive Restart (AR) to dampen oscillations and speed up optimization. Adaptive Restart resets the velocity, $\mathbf{v} = \mathbf{0}$, when $\mathbf{g}^T \cdot \mathbf{v} < 0$ which can be viewed as a measure of alignment. AB also measures alignment using cosine similarity but applies a continuous correction to \mathbf{g} rather than a discrete reset of \mathbf{v} . This makes AB more applicable in a noisy optimization setting such as SGD. Periodically resetting the step direction is also used in nonlinear conjugate gradient optimization methods. Adaptive Braking can be seen as a form of nonlinear conjugate gradient optimization since the step direction accumulation is adaptively adjusted based on the current gradient. There are many variations of nonlinear conjugate gradient optimization but to the best of our knowledge, none of these forms are exactly equivalent to Adaptive Braking.

The rest of this section shows the algorithmic details of the methods we compare against in our experiments.

A.1. Asynchronous SGD (ASGD)

Algorithm 1 Momentum-ASGD: worker j

Always do:
 Receive parameters \mathbf{w}_{t-D} from the master
 Compute gradient: $\mathbf{g}_{t;j} = G(\mathbf{w}_{t-D})$
 Send $\mathbf{g}_{t;j}$ to the master

Algorithm 2 Momentum-ASGD: master

For $t = 1 \dots T$ do:
 Receive gradient $\mathbf{g}_{t;j}$ from worker j
 Update momentum: $\mathbf{v}_{t+1} = m\mathbf{v}_t + \mathbf{g}_{t;j}$
 Update master’s weights: $\mathbf{w}_{t+1} = \mathbf{w}_t - \eta_t \mathbf{v}_{t+1}$
 Send \mathbf{w}_{t+1} to worker j

A.2. Staleness-Aware

Staleness-Aware divides the original learning rate by the delay of the current gradient in each update step.

Algorithm 3 Staleness-Aware: master

Initialize an iteration array: $iter = [0] * N$
 For $t = 1 \dots T$ do:
 Receive gradient $\mathbf{g}_{t;j}$ from worker j
 Calculate worker j ’s delay: $D_t = t - iter[j]$
 Update momentum: $\mathbf{v}_{t+1} = m\mathbf{v}_t + \mathbf{g}_{t;j}$
 Update master: $\mathbf{w}_{t+1} = \mathbf{w}_t - \frac{\eta_t}{D_t} \mathbf{v}_{t+1}$
 Send \mathbf{w}_{t+1} to worker j
 Save current iteration: $iter[j] = t$

A.3. Shifted Momentum

Shifted Momentum assigns an independent velocity $\mathbf{v}_{t;j}$ to each worker j , and updates the master weights using the current worker’s velocity.

Algorithm 4 Shifted Momentum: worker j

Always do:
 Receive parameters \mathbf{w}_{t-D} from the master
 Compute gradient: $\mathbf{g}_{t;j} = G(\mathbf{w}_{t-D})$
 Update momentum $\mathbf{v}_{t+1;j} = m\mathbf{v}_{t;j} + \mathbf{g}_{t;j}$
 Send $\mathbf{v}_{t+1;j}$ to the master

Algorithm 5 Shifted Momentum: master

For $t = 1 \dots T$ do:
 Receive gradient $\mathbf{v}_{t+1;j}$ from worker j
 Update master’s weights: $\mathbf{w}_{t+1} = \mathbf{w}_t - \eta_t \mathbf{v}_{t+1;j}$
 Send \mathbf{w}_{t+1} to worker j

A.4. DANA

DANA assigns an independent velocity $v_{t,j}$ to each worker j , and computes the gradient on estimated future weights.

Algorithm 6 DANA: worker j

Always do:

- Receive parameters $\hat{\mathbf{w}}_{t-D}$ from the master
 - Compute gradient: $\mathbf{g}_{t,j} = G(\mathbf{w}_{t-D})$
 - Update momentum: $\mathbf{v}_{t+1,j} = m\mathbf{v}_{t,j} + \mathbf{g}_{t,j}$
 - Send $\mathbf{v}_{t+1,j}$ to the master
-

Algorithm 7 DANA: master

For $t = 1 \dots T$ do:

- Receive gradient $\mathbf{v}_{t+1,j}$ from worker j
 - Update master’s weights: $\mathbf{w}_{t+1} = \mathbf{w}_t - \eta_t \mathbf{v}_{t+1,j}$
 - Estimates future weights: $\hat{\mathbf{w}}_{t+1} = \mathbf{w}_t - \eta_t m \sum_j \mathbf{v}_{t+1,j}$
 - Send $\hat{\mathbf{w}}_{t+1}$ to worker j
-

A.5. Delay-Compensated ASGD

Delay-Compensated ASGD approximates the Hessian of the loss surface and corrects the delayed gradient based on the weight inconsistency.

Algorithm 8 Delay-Compensated ASGD: master

For $t = 1 \dots T$ do:

- Receive gradient $\mathbf{g}_{t,j}$ from worker j
 - Compensate gradient: $\hat{\mathbf{g}}_{t,j} = \mathbf{g}_{t,j} + \nabla \mathbf{g}_{t,j} \cdot (\mathbf{w}_t - \mathbf{w}_{t-D})$
 - Update momentum: $\mathbf{v}_{t+1} = m\mathbf{v}_t + \hat{\mathbf{g}}_{t,j}$
 - Update master’s weights: $\mathbf{w}_{t+1} = \mathbf{w}_t - \eta_t \mathbf{v}_{t+1}$
 - Send \mathbf{w}_{t+1} to worker j
-

where $\nabla \mathbf{g}_{t,j}$ is approximated with $\lambda_t \cdot \text{diag}(\mathbf{g}_{t,j} \odot \mathbf{g}_{t,j})$ and λ_t is the variance control parameter, set using a moving-average as described in the original paper. We note that this algorithm is modified to work with SGDM.

A.6. Adaptive Braking

Algorithm 9 Adaptive Braking: master

For $t = 1 \dots T$ do:

- Receive gradient $\mathbf{g}_{t,j}$ from worker j
 - For i in parameter groups do:
 - Compute braking: $\alpha_t^i = 1 - \rho \cos \angle(\mathbf{g}_t^i, \mathbf{v}_t^i)$
 - Update momentum: $\mathbf{v}_{t+1}^i = m\mathbf{v}_t^i + \alpha_t^i \mathbf{g}_{t,j}^i$
 - Update master’s weights: $\mathbf{w}_{t+1}^i = \mathbf{w}_t^i - \eta_t \mathbf{v}_{t+1}^i$
 - Send \mathbf{w}_{t+1} to worker j
-

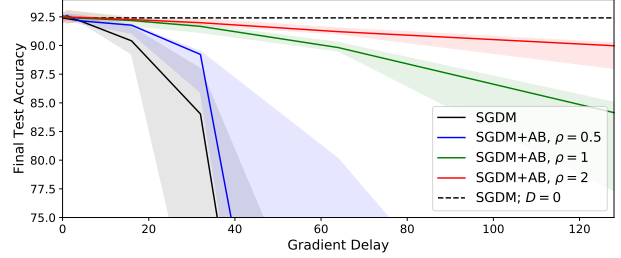


Figure 6. ResNet-20 + CIFAR-10 final test accuracy for different delays. Adaptive Braking improves the delay tolerance of SGDM when training in an ASGD setting.

B. Hyperparameter Settings

The per-worker hyperparameter settings used in our neural network training experiments are listed in Table 2. For CIFAR-10, we choose to use a small batch size of 32 rather than the standard setting of 128 to showcase a training setup with high momentum, which is where Adaptive Braking is most effective. For ImageNet-1k we use a per-worker batch size of 32 to reflect a common SSGD training setup with 8 GPUs and a total batch size of 256, and choose a momentum of 0.99 based on hyperparameter searches performed by Shallue et al. (2019). For DC we use the adaptive form of the algorithm and adopt the original paper’s hyperparameters. The other mitigation strategies are hyperparameter-free.

Table 2. Single-worker hyperparameter settings used for ASGD experiments.

PARAMETER	CIFAR-10	IMAGENET1K
MODEL ARCHITECTURE	RESNET-20	RESNET-50
PER-WORKER BATCH SIZE	32	32
INITIAL LEARNING RATE (η)	0.01	0.0125
MOMENTUM (m)	0.95	0.99
WEIGHT DECAY (λ)	5E-4	1E-4
EPOCHS	[100, 50, 50, 50]	[30, 30, 20, 10]
LR DECAY	0.1	0.1
LR WARMUP EPOCHS	0	5

C. CIFAR-10 Extended Results

In Figure 6, we simulate asynchronous training of ResNet-20 on CIFAR-10 and measure the delay tolerance of SGDM with or without Adaptive Braking. Each experiment is repeated 5 times and the median final test accuracy is plotted.

We find that AB greatly improves the delay tolerance of SGDM. In particular, we can train asynchronously with a gradient delay of $D = 32$ with only a -0.42% drop in test accuracy. Even at extreme settings with $D = 128$, the degradation is only -2.43%, while vanilla SGDM fails to converge at all. We also find that the delay tolerance improves as ρ is increased from 0.5 to 2.0.

In Table 3 we list extended results with more settings of brak-

Table 3. ResNet-20 + CIFAR-10 final test accuracy, trained with different delays D . The training hyperparameters are listed in Table 2. Each reported accuracy is a median over 5 trials. For each trial, we use the median test accuracy over the last 10 epochs of training.

ALGORITHM	D=0	D=1	D=4	D=16	D=32	D=64	D=128
SGDM	92.41%	92.34%	92.16%	90.41%	84.03%	10.09%	10.00%
SGDM+AB, $\rho = 0.5$	92.36%	92.61%	92.16%	91.78%	89.22%	25.25%	45.11%
SGDM+AB, $\rho = 1$	92.61%	92.51%	92.39%	92.18%	91.67%	89.82%	84.15%
SGDM+AB, $\rho = 2$	92.47%	92.43%	92.46%	92.27%	91.99%	91.21%	89.98%
SGDM+AB, $\rho = 3$	92.44%	92.44%	92.54%	91.87%	91.82%	90.69%	88.22%
SGDM+AB, $\rho = 4$	92.12%	91.98%	92.07%	91.57%	91.50%	90.87%	90.07%
SGDM+AB, $\rho = 5$	92.12%	91.94%	92.01%	90.97%	90.41%	89.35%	87.06%

ing coefficient ρ . The results suggest that larger ρ should be used for larger delays. The choice of $\rho = 2$ is the most consistent across $D = [0, 1, 4, 16, 32, 64, 128]$, performing best or second-best in almost all delay settings.

D. Parameter Grouping for AB

The AB gradient scaling factor α_t^i is non-linear with respect to \mathbf{g}_t^i and \mathbf{v}_t^i , and depends on the granularity with which the model parameters are grouped. We consider three levels of granularity for grouping:

- **Per tensor:** This is based on the default grouping of parameters into tensors in PyTorch. In this case each convolutional or linear layer has a weight tensor which contains all the multiplicative weights and optionally a bias which is a separate tensor. Normalization layers have their own bias and scaling tensors.
- **Per filter:** Here the weights of each neuron or filter are treated separately. The biases and other parameters such as those in the normalization layers are still grouped per tensor.
- **Per element:** Here each parameter is treated separately, and the scaling coefficient reduces to $\alpha_t^i = 1 - \rho \operatorname{sgn}(g_t^i \cdot v_t^i)$.

In Table 4 we find that using a filter-wise grouping of parameters leads to the best performance for ResNet-20 trained on CIFAR-10, even when accounting for different optimal settings of ρ for each grouping method. Therefore we use filter-wise Adaptive Braking for all of our experiments.

E. AB with Weight Decay

When weight decay is used with Adaptive Braking, we add the weight decay term to the velocity independently, and do not consider the weight decay to be part of the gradient when computing the cosine similarity:

$$\alpha_t^i = 1 - \rho \frac{\langle \mathbf{g}_t^i, \mathbf{v}_t^i \rangle}{\max(\|\mathbf{g}_t^i\|, \|\mathbf{v}_t^i\|, \epsilon)} \quad (6)$$

$$\approx 1 - \rho \cos \angle(\mathbf{g}_t^i, \mathbf{v}_t^i)$$

$$\mathbf{v}_{t+1}^i = m\mathbf{v}_t^i + \alpha_t^i \mathbf{g}_t^i + \lambda \mathbf{w}_t^i \quad (7)$$

$$\mathbf{w}_{t+1}^i = \mathbf{w}_t^i - \eta \mathbf{v}_{t+1}^i \quad (8)$$

This helps prevent α_t^i from being skewed by the weight decay term, which is correlated across steps.

F. AB compared with DC

Under a particular approximation, delay-compensated ASGD has a similar form to Adaptive Braking. DC attempts to correct the delayed gradient \mathbf{g}_t by measuring the change in the master weights, and using a Hessian approximation to estimate the up-to-date gradient $\hat{\mathbf{g}}_t$ at the current master weights:

$$\mathbf{g}_t = G(\mathbf{w}_{t-D}) \quad (9)$$

$$\hat{\mathbf{g}}_t = G(\mathbf{w}_t) \approx \mathbf{g}_t + \lambda \mathbf{H}_t \cdot (\mathbf{w}_t - \mathbf{w}_{t-D}) \quad (10)$$

$$\approx \mathbf{g}_t + \lambda (\mathbf{g}_t \cdot \mathbf{g}_t^T) \cdot (\mathbf{w}_t - \mathbf{w}_{t-D}) \quad (11)$$

$$\approx \mathbf{g}_t + \lambda \cdot \operatorname{diag}(\mathbf{g}_t \odot \mathbf{g}_t) \cdot (\mathbf{w}_t - \mathbf{w}_{t-D}) \quad (12)$$

$$= \mathbf{g}_t + \lambda (\mathbf{g}_t \odot \mathbf{g}_t) \odot (\mathbf{w}_t - \mathbf{w}_{t-D}) \quad (13)$$

Table 4. ResNet-20 + CIFAR-10 final test accuracy, trained with a delay of $D = 32$. Filter-wise grouping outperforms tensor- or element-wise grouping. The optimal setting of ρ for each method is highlighted.

ALGORITHM	TENSOR	FILTER	ELEMENT
SGDM+AB, $\rho = 0.25$	88.70%	85.46%	88.20%
SGDM+AB, $\rho = 0.5$	87.50%	89.24%	90.35%
SGDM+AB, $\rho = 1$	91.38%	91.67%	89.54%
SGDM+AB, $\rho = 2$	91.71%	92.14%	88.97%
SGDM+AB, $\rho = 4$	91.43%	91.15%	88.22%

Zheng et al. (2017) use the Taylor Series expansion of the delayed gradient but truncate higher order terms (10). \mathbf{H}_t is the hessian at time t , and λ is a hyperparameter used to control the strength of the second-order correction. They then approximate $\mathbf{H}_t \approx \mathbf{g}_t \cdot \mathbf{g}_t^T \approx \text{diag}(\mathbf{g}_t \odot \mathbf{g}_t)$ which makes the compensation method an element-wise operation. To arrive at AB, we maintain the outer-product form (11) for the remainder of this section.

During SGDM training, the weight update at each step t is $-\eta \mathbf{v}_t$. If we assume the velocity over the last D steps is relatively unchanged, then we can approximate the total weight change from step $(t - D)$ to step t as:

$$\mathbf{w}_t - \mathbf{w}_{t-D} = - \sum_{i=0}^{D-1} \eta \mathbf{v}_{t-i} \quad (14)$$

$$\approx - \sum_{i=0}^{D-1} \eta \mathbf{v}_t \quad (15)$$

$$= -\eta D \mathbf{v}_t \quad (16)$$

Substituting this approximation into (11), we end up with a gradient scaling term that involves a dot product of the gradient and the velocity:

$$\hat{\mathbf{g}}_t \approx \mathbf{g}_t + \lambda (\mathbf{g}_t \cdot \mathbf{g}_t^T) \cdot (-\eta D \mathbf{v}_t) \quad (17)$$

$$= \mathbf{g}_t (1 - \lambda \eta D (\mathbf{g}_t^T \cdot \mathbf{v}_t)) \quad (18)$$

$$= \mathbf{g}_t (1 - \lambda' (\mathbf{g}_t^T \cdot \mathbf{v}_t)) \quad (19)$$

Finally, we can use an adaptive setting of λ' , normalizing by the magnitudes of the gradient and velocity at time t . At this point we are no longer approximating the master weight gradient $\hat{\mathbf{g}}_t$, so we adjust notation:

$$\lambda'_t = \frac{\lambda'_0}{\|\mathbf{g}_t\| \cdot \|\mathbf{v}_t\|} \quad (20)$$

$$\mathbf{g}'_t = \mathbf{g}_t (1 - \lambda'_0 \cos \angle(\mathbf{g}_t, \mathbf{v}_t)) \quad (21)$$

The gradient scaling term in (21) is now exactly $\alpha_t = 1 - \rho \cos \angle(\mathbf{g}_t, \mathbf{v}_t)$ used for AB. Note that for AB the braking coefficient ρ is chosen independently rather than set based on the learning rate η and delay D .

G. Gradient scale α and braking coefficient ρ

The strength of AB's gradient scaling α_t^i depends on the choice of braking coefficient ρ . In general, the optimal setting of ρ is task-dependent and can be optimized as a hyperparameter, but we find that values in $\rho \in [0.5, 2]$ work

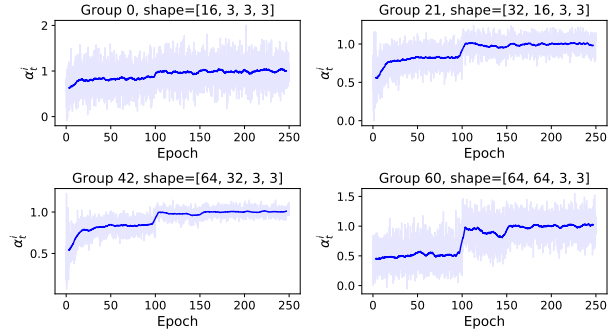


Figure 7. The average gradient scaling α_t^i increases throughout training. This plot measures α_t^i for four different convolutional layers in ResNet-20. The model is trained on CIFAR-10 with SGDM+AB, $\rho = 2$, with a delay of $D = 32$.

well across different delays and model architectures. Note that if ρ is set larger than 1, it is possible for the gradient scaling at a particular step to be negative, but we find this to rarely happen in practice. We have also experimented with clamping α_t^i to be non-negative but do not see a significant effect on convergence, so for simplicity we do not perform clamping in the standard form of AB.

In Figure 7, we measure the gradient scaling α_t^i applied by Adaptive Braking during ResNet-20 + CIFAR-10 training. At the start of training, successive gradients are well-aligned, so as expected α_t^i is less than one and AB scales down the gradients. In the later stages of training, successive gradients are not well aligned and α_t^i returns closer to 1, which would be equivalent to vanilla SGDM.

We also find that the gradient scaling rarely becomes negative, despite the fact that we are using a braking coefficient of $\rho = 2$. This confirms that even though the potential range of the gradient scaling is $1 - \rho \leq \alpha_t^i \leq 1 + \rho$, the typical values seen during CNN training rarely reach such extreme values. This is probably due to the high dimensionality of the parameter groups, which leads the average cosine similarity to be closer to zero.

The norm of the gradient is also usually smaller than the norm of the velocity ($\tau_t^i < 1$), so even if α_t^i does become negative at an individual step, it will likely only reduce the velocity norm, not completely reverse the direction of optimization (gradient ascent). In extreme cases such as a loss plane with constant gradient, we would see oscillations if $\rho > 1$. But again, we do not see this behavior in practice when training CNNs.

H. Velocity Norm and Gradient Velocity Ratio

AB tends to reduce or remove the growth in the velocity that happens if successive gradients are well aligned. This is a pervasive problem in delayed gradient training, especially

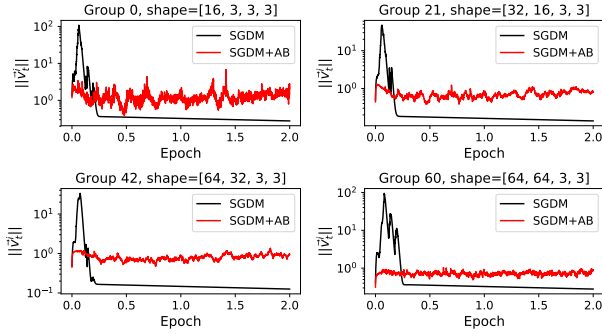


Figure 8. At the very start of training, SGDM+AB scales down similarly-aligned gradients, and prevents a blowup of the velocity norm that occurs with vanilla SGDM. Each plot measures $\|\mathbf{v}^i\|$ for a different group of convolutional layer weights \mathbf{w}^i in ResNet-20. The y-axis is log scaled. The model is trained on CIFAR-10 with a delay of $D = 32$.

at the very start of training where the first $\approx D$ gradient estimates are computed on the same initial weights. In Figure 8, we plot a fine-grained view of $\|\mathbf{v}_t^i\|$ at the very start of ResNet-20 + CIFAR-10 training. We train with either SGDM (black) or SGDM+AB (red) and use a constant delay of $D = 32$. Without AB, the velocity norm across many parameter groups explodes within the first few hundred steps. This means that the gradients are well aligned and sum constructively, leading to large $\|\mathbf{v}^i\|$. When AB is used, this initial blowup is greatly reduced.

As training continues, we notice that the average magnitude of $\|\mathbf{v}_t^i\|$ is not very different between SGDM and SGDM+AB, and can often be higher when using SGDM+AB (See Figure 9). So even though Adaptive Braking is scaling down the gradient, and limiting the growth of the velocity, AB does not significantly decrease the average velocity norm $\|\mathbf{v}^i\|$. Instead, AB actually stabilizes the velocity and leads the optimizer to take larger steps in early training than it would with vanilla SGDM.

This suggests that replacing Adaptive Braking with a smaller learning rate would not produce the same benefits. Slowing down the growth of the velocity vector is not the same as reducing the magnitude of the weight updates. This idea is explored further in Appendix J.

To better measure the effect of AB across different layers and across the training schedule, we introduce Gradient Velocity Ratio (GVR), which measures the ratio of the gradient norm over the velocity norm for a group i of parameters:

$$\tau_t^i = \frac{\|\mathbf{g}_t^i\|}{\|\mathbf{v}_t^i\|} \quad (22)$$

We believe GVR is a good measure of a momentum-based

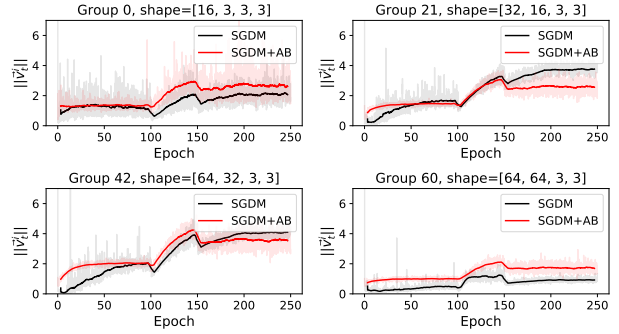


Figure 9. The velocity norm $\|\mathbf{v}_t^i\|$ measured across a full training run, for four different convolutional layers in ResNet-20. During early training, the velocity norm is larger when using SGDM+AB than when using vanilla SGDM. The model is trained on CIFAR-10 with a delay of $D = 32$.

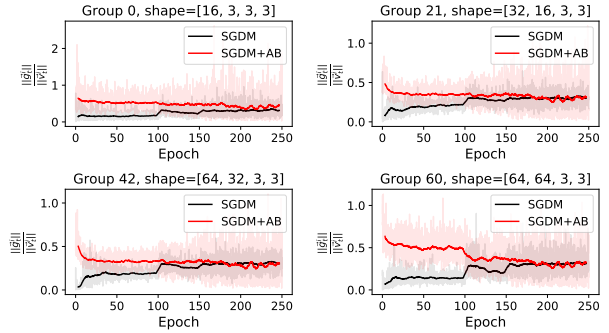


Figure 10. The GVR $\tau_t^i = \|\mathbf{g}_t^i\|/\|\mathbf{v}_t^i\|$ is higher when training with SGDM+AB than with vanilla SGDM. Each plot measures $\|\mathbf{v}^i\|$ for a different group of convolutional layer weights \mathbf{w}^i . The model is trained on CIFAR-10 with a delay of $D = 32$.

optimizer’s ability to change its trajectory. We measure the GVR τ_t^i during training in Figure 10, and find that using AB greatly increases GVR throughout training. This supports our theory that Adaptive Braking makes it easier to change the direction of the optimization trajectory during ASGD training.

I. Weight Update Direction

The instantaneous effect of AB on the SGDM weight update is to make the weight update more aligned with the gradient when the gradient and velocity directions disagree. This effect is illustrated in Figure 11, where we compare the alignment of the gradient with the weight update for both SGDM and SGDM+AB, $\rho = 2$. We plot measurements for a range of gradient-velocity ratio (GVR) values $\tau = [0.1, 0.2, 0.5, 0.8]$ which we find is typical in CNN training (See Appendix H and Figure 10).

Note that a similar effect can be achieved for vanilla SGDM if we significantly reduce the momentum m : for instance if

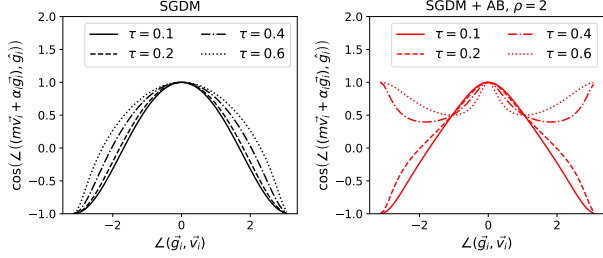


Figure 11. Alignment of weight update with gradient, as a function of alignment of gradient and velocity. When the direction of \mathbf{g}^i disagrees with the direction of \mathbf{v}^i , the SGDM + AB weight update is closer to \mathbf{g}^i .

$m = 0$ then the weight update is always perfectly aligned with the gradient. When training with delayed gradients and no mitigation, setting $m = 0$ is a valid choice and can even be optimal when there is no gradient noise. However we find that in both the convex quadratic and neural network ASGD setting that we can achieve faster convergence if we use nonzero momentum combined with delay mitigation. This is why AB’s ability to reorient the weight update in the presence of momentum is valuable.

J. AB Ablation Study

Since AB scales the gradient during both the velocity update step and the weight update step, we can ask whether the delay tolerance of AB comes from just the instantaneous correction to the weight update, or from the long-term effect on the velocity. The two effects are made clear by looking at an unwrapped version of the SGDM+AB update equations:

$$\mathbf{v}_{t+1}^i = m\mathbf{v}_t^i + \alpha_t^i \mathbf{g}_t^i \quad (23)$$

$$\mathbf{w}_{t+1}^i = \mathbf{w}_t^i - \eta (m\mathbf{v}_t^i + \alpha_t^i \mathbf{g}_t^i) \quad (24)$$

For SGDM, the scaling factor α_t^i is always fixed to 1. For SGDM+AB, α_t^i is normally computed per-step as described by (3) and applied in both equations. Alternatively, we can apply the scaling in only one equation or the other.

If we choose to apply gradient scaling only on the velocity update, we call this algorithm AB-vel-only, with update equations:

$$\mathbf{v}_{t+1}^i = m\mathbf{v}_t^i + \alpha_t^i \mathbf{g}_t^i \quad (25)$$

$$\mathbf{w}_{t+1}^i = \mathbf{w}_t^i - \eta (m\mathbf{v}_t^i + \mathbf{g}_t^i) \quad (26)$$

If we choose to apply gradient scaling only on the weight update, we call this algorithm AB-weight-only, with update equations:

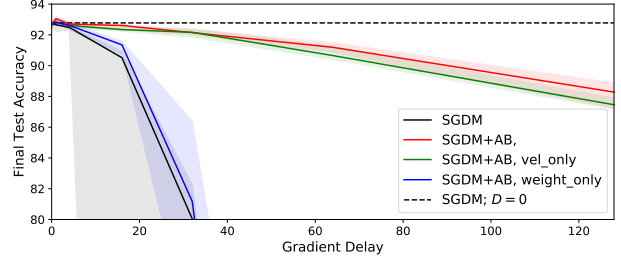


Figure 12. Scaling the gradient during the velocity update is more important for delay tolerance than scaling the gradient during the weight update.

$$\mathbf{v}_{t+1}^i = m\mathbf{v}_t^i + \mathbf{g}_t^i \quad (27)$$

$$\mathbf{w}_{t+1}^i = \mathbf{w}_t^i - \eta (m\mathbf{v}_t^i + \alpha_t^i \mathbf{g}_t^i) \quad (28)$$

In Figure 12, we measure the delay tolerance of SGDM with either AB-vel-only or AB-weight-only. We find that most of the delay tolerance of AB comes from scaling the gradient before updating the velocity. This supports the theory that balancing the velocity norm and dampening oscillations is crucial to mitigating delays.

K. Extended Noisy Quadratic Model Analysis

K.1. Problem Setup

We assume that the convex quadratic is centered and aligned with the axis. This can be done without a loss of generality since the optimizers considered are both translation and rotation-invariant². We write the loss as:

$$\mathcal{L}(\mathbf{w}) = \frac{1}{2} \mathbf{w}^T \mathbf{H} \mathbf{w} = \frac{1}{2} \sum_{k=1}^N \lambda_k w_k^2 \quad (29)$$

where $\mathbf{w} = [w_1, \dots, w_N]^T$ are the weights to be optimized and $\mathbf{H} = \text{diag}(\lambda_1, \dots, \lambda_N)$ is the Hessian of the loss.

Following Zhang et al. (2019) we assume additive gradient noise with covariance equal to the Hessian of the loss. We also adopt their Hessian eigenvalue spectrum which is of the form $\{\frac{1}{j}\}_{j=1}^N$ with $N = 10^4$ which they show can closely match certain neural networks. We write the gradient at timestep t as:

$$\mathbf{g}_t = \mathbf{H} \mathbf{w}_{t-D} + \sigma \mathcal{N}(\mathbf{0}, \mathbf{H}) \quad (30)$$

where \mathbf{w}_{t-D} are the weights with delay D , $\mathcal{N}(\mathbf{0}, \mathbf{H})$ is the multivariate normal distribution noise with mean $\mathbf{0}$ and covariance matrix \mathbf{H} , and σ scales the noise.

²To make AB rotation-invariant we use a single group spanning all parameters. We investigate different groupings in Appendix D.

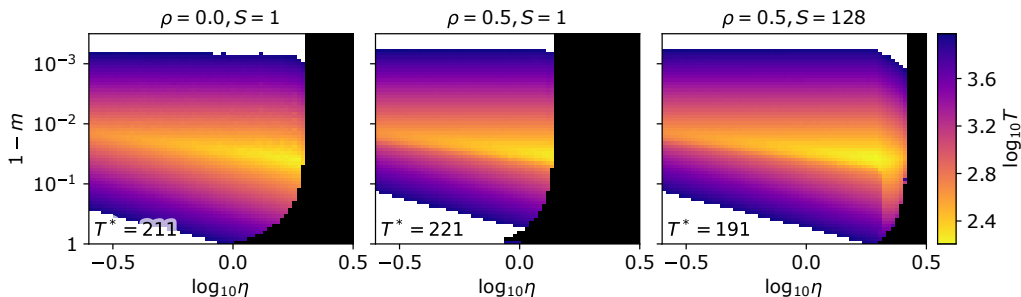


Figure 13. This figure shows the effect of micro-stepping on the convergence region in the first row of Figure 1. Only high learning rates are shown and 10000 steps are performed. With micro-stepping AB increases the stability region compared to plain SGDM and unlocks faster trajectories.

Zhang et al. (2019) use the noisy quadratic model to explore the effects of batch size (simulated by modifying the noise scale σ) with good predictive results for neural networks. Their focus is on linear optimizers which allows them to derive closed form solutions for the convergence. Since AB is non-linear and has a cross-feature dependency we explicitly carry out the optimization on the full quadratic and do not use any sort of binning of similar eigenvalues. The objective of the optimization is to bring the loss below the target loss $\varepsilon = 0.01$ and the weights are initialized to $\mathbf{w} = \mathbf{1}$. We measure the quality of trajectories with the number of steps, T , required to reach the target loss.

K.2. Energy Measure

In Section 3 we explore the effect of AB on individual components. To do this effectively we introduce an energy measure to estimate the convergence of individual components and compare it between states. Using the loss for this is problematic because it oscillates and a low loss does not necessarily indicate convergence (if the velocity is large). In more realistic settings we can not easily determine what the components are and therefore can not compute component losses, apply different learning rates to different components or early stop individual components. We use a similar energy model as Hermans & Louppe (2018) that accounts for both the loss (potential energy) and velocity (kinetic energy). Our energy (E) is normalized with the learning rate (η) making it directly comparable with the loss:

$$E_t = \mathcal{L}(\mathbf{w}_t) + \frac{1}{2} \frac{\|\mathbf{w}_t - \mathbf{w}_{t-1}\|^2}{\eta} \quad (31)$$

$$= \mathcal{L}(\mathbf{w}_t) + \frac{1}{2} \eta \|\mathbf{v}_t\|^2 \quad (32)$$

Note that the energy upper bounds the loss so an energy of zero would mean that a component has fully converged. For an oscillating trajectory the energy is roughly equal to the loss at the extreme points where the velocity is approximately zero. Overall the energy can be viewed as roughly estimating the envelope of the loss for an oscillating component. This makes it easier to estimate convergence from a

single state and compare the convergence of different states than using the loss directly.

Algorithm 10 AB with micro-stepping

```

For t = 1...T do:
  Compute gradient  $\mathbf{g}$ 
   $\mathbf{v} \leftarrow m\mathbf{v}$ 
  For i = 1...S do:
     $\alpha \leftarrow 1 - \rho \frac{\langle \mathbf{g}, \mathbf{v} \rangle}{\max(\|\mathbf{g}\|, \|\mathbf{v}\|, \varepsilon)}$ 
     $\mathbf{v} \leftarrow \mathbf{v} + \frac{\alpha}{S} \mathbf{g}$ 
   $\mathbf{w} \leftarrow \mathbf{w} - \eta \mathbf{v}$ 
    
```

K.3. Micro-stepping

Figure 1 shows that in the no-delay and no-noise case AB can slightly reduce the region of stability. This leads to slightly worse optimal trajectories. In Section 3 we state that this happens because AB can magnify certain high frequency oscillations. With noise and delays this does not seem to be an issue, potentially because the baseline SGDM trajectories don't converge to the target loss for hyperparameter settings where high frequency oscillations could occur.

As an example of AB magnifying oscillations, consider the case where AB is applied on a single component with curvature λ , learning rate $\frac{1}{\lambda} < \eta < \frac{2}{\lambda}$ and very small momentum value $m \approx 0$. This will result in a trajectory that overshoots the minimum at every step and \mathbf{g} and \mathbf{v} will always be oppositely aligned. This causes AB to apply a constant $\alpha = 1 + \rho$, effectively increasing the learning rate, potentially causing instability.

The issue arises from AB over-correcting the velocity when the gradient \mathbf{g}_t and velocity \mathbf{v}_t are oppositely aligned. This happens because AB scales the gradient based on the alignment of \mathbf{v}_t and \mathbf{g}_t without considering the resulting alignment of \mathbf{g}_t and \mathbf{v}_{t+1} . In cases where $\|\mathbf{v}_t\|$ is small and \mathbf{g}_t and \mathbf{v}_{t+1} are oppositely aligned this can lead to larger $\|\mathbf{v}_{t+1}\|$. Various forms of clamping can help here, for example enforcing $\alpha \leq 1$ but we have found that this can reduce

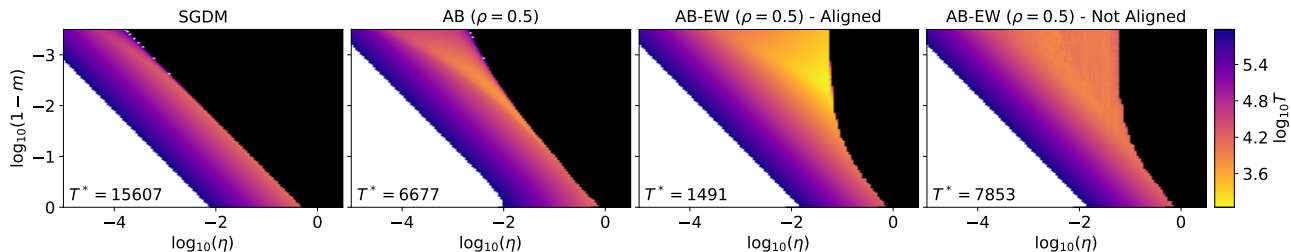


Figure 14. Convergence heatmaps for the optimization of a low dimensional convex quadratic (CQ) with a delay of one. Plain SGDM and standard AB are rotation invariant but applying AB element-wise is not. Element-wise AB performs very well if the axes of the CQ are aligned, such that the AB is applied to each component individually (third panel). The last panel shows element-wise AB for a CQ with a random alignment. In this case applying AB element-wise does not work as well as the global form, although the region of stability is larger.

the effectiveness of AB.

Another way is to change the velocity update to consider more than just the initial alignment of \mathbf{g}_t and \mathbf{v}_t . We can divide the velocity update into S “micro-steps”, calculating a different α for each one as shown in Algorithm 10. For large values of S micro-stepping might have significant overhead but could help AB in the large batch size or low noise settings. Figure 13 shows the effects of micro-stepping on the speed of convergence. It shows that with micro-stepping AB can tolerate higher learning rates than plain SGDM and slightly decreases the minimum steps needed to reach the target loss.

K.4. Parameter Grouping

Adaptive Braking operates by computing an alignment score between the gradient and velocity for a group of parameters and then scaling the gradient based on the alignment. The performance of AB depends on the choice of groups. For neural networks we find that filter-wise grouping works well, see Appendix D. In this section we explore the effect of grouping for convex quadratics, in particular we compare the global form (with a single group) to the element-wise form.

To decrease compute requirements we use low dimensional models in this section. We use 32 components with a log-uniform eigenvalue spectrum from 10^{-4} to 1 and a target loss of $\epsilon = 10^{-5}$. Figure 14 shows the steps required to reach the target loss for different AB forms for a delay of 1 and no noise. We can see that the global form of AB outperforms the baseline. The element-wise form works really well if the quadratic aligns with the axes. In this case it is really performing component-wise AB. This can speed up the convergence of all components that are sufficiently underdamped. For overdamped components this slows their convergence (by effectively lowering the learning rate). However, since all components are stabilized, higher learning rates can be used which at least partially compensates for this effect. Ideally we could apply AB selectively to the components that need to be dampened

without affecting the other ones. Unfortunately we generally don’t know what the components are and element-wise AB does not necessarily outperform the global form of AB for a random alignment (see Figure 14).

Overall there seems to be a trade-off in the group size. Each additional component in a group lowers the correlation of the scaling to the other components, weakening the dampening effect. Using a larger number of groups, with fewer components each, may give stronger correlations increasing the dampening effect. Ideally the most unstable components should fall in separate groups so they can be dampened effectively. It may also be important for components to be contained within a single group. If this is not the case, different coordinates of the gradient for a given component may be scaled differently. This effectively rotates the gradient, potentially causing it to interfere with the convergence of other components. This might be why element-wise AB generally doesn’t perform as well as using larger groups (when the loss is not aligned as is usually the case). The filter-wise grouping we use for neural networks (see Appendix D) could strike a good balance between the number of groups and splitting components between groups.